CONSTRUCTION OF ADAPTIVE WAVELETS USING UPDATE LIFTING AND QUADRATIC DECISION CRITERIA

*Béatrice Pesquet-Popescu**

ENST, Signal and Image Proc. Dept.,
46, rue Barrault, 75634 Paris, France
Beatrice.Pesquet@enst.fr

Gemma Piella† *and Henk Heijmans*

CWI, Kruislaan 413, 1098 SJ Amsterdam
The Netherlands
Gemma.Piella, Henk.Heijmans@cwi.nl

ABSTRACT

This paper studies lifting schemes that are adaptive with respect to the gradient vector of the input signal and require no overhead information for perfect reconstruction. The choice of the update filter is triggered by a binary decision criterion based on a weighted ℓ^2-type seminorm of the gradient. Such an adaptive scheme has great potential for preserving the discontinuities in signals and images and providing a compact data representation, as illustrated by some simulation examples.

1. INTRODUCTION

Wavelet representations provide a powerful tool for the analysis of signals and images. The multiresolution analysis deriving from a classical linear wavelet transform, however, leads to a uniform smoothing of the image contents when going to lower resolutions. However, in a large number of applications in signal and image processing it would be useful to have wavelet decompositions that leave intact or even enhance certain important signal characteristics such as sharp transitions, edges, or, any other singularity. The importance of such "intelligent" representations in image analysis, compression, denoising, or feature extraction, has been recognized by various researchers and has lead to a wealth of new approaches in wavelet theory (bandelets [1], ridgelets [2], curvelets [3], nonlinear [4] and morphological wavelets [5], etc.).

A very promising technique among these nonlinear representations consists in building wavelet-like decompositions using simple FIR filters, that adapt themselves to the signal or image to be analysed. However, one of the notorious drawbacks of such adaptive schemes is the overhead represented by the additional data that is required to "remember" which filter has been used at each location. In [6], a new framework based on an adaptive lifting scheme has been provided for building perfect reconstruction filter banks, which *do not require any additional bookkeeping* to enable inversion. In this paper, we follow this approach and provide a new construction, based on a quadratic form criterion driving the non-linear decision step.

The paper is organized as follows: in the next section we recall the construction of adaptive lifting schemes that do not require bookkeeping. In Section 3 we introduce the quadratic decision criterion and provide the conditions on the update filters for perfect reconstruction. The form of the update filters and some interesting particular cases are also studied. Simulation results and concluding remarks are presented in the last two sections.

2. ADAPTIVE UPDATE LIFTING

Let us denote the input signal by $x_0(n)$, $n \in \mathbb{Z}$, and its polyphase components respectively by $x(n) = x_0(2n)$ and $y(n) = x_0(2n+1)$. In the classical lifting scheme [7], the update filter, as well as the corresponding addition operation, is fixed. Here, our starting point is the adaptive scheme proposed in [6], where these operations depend on the properties of the input signal. In this approach, a binary decision map triggering the choice of the update filter is constructed based on the *gradient information* and the update operator is selected according to this map (see Fig. 1).

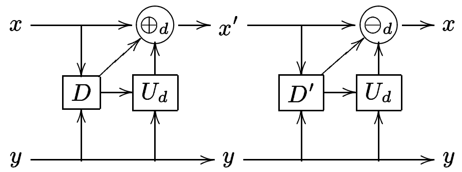

Fig. 1. Adaptive update lifting scheme.

More precisely, if d_n is the binary decision at location n, then the updated value $x'(n)$ is given by

$$x'(n) = x(n) \oplus_{d_n} U_{d_n}(y)(n)\,. \qquad (1)$$

*The work of the first and third author is partially supported by the IST Programme of the EU under contract number IST-2000-26467 (MASCOT).

†The work of the second author is supported by the Dutch Technology Foundation STW, project no. CWI 4616.

In this structure, we have a great flexibility in the choice of the "addition" $\oplus_d$, as well as the update filter $U_d(y)$ for the values $d = 0, 1$. Henceforth we assume that the addition $\oplus_d$ is the following invertible operator:

$$x \oplus_d u = \alpha_d(x + u), \quad \text{with } \alpha_d \neq 0. \qquad (2)$$

The update filter is defined as follows

$$U_{d_n}(y)(n) = \sum_{j=-L_1}^{L_2} \lambda_{d_n,j} y_j(n) , \qquad (3)$$

where $y_j(n) = y(n + j)$ and L_1, L_2 are nonnegative integers. Unless otherwise stated, $\sum_j$ will stand for $\sum_{j=-L_1}^{L_2}$ in this paper. Note that the filter coefficients $\lambda_{d_n,j}$ depend on the decision d_n in each point n. From (1) and (3), we deduce the update equation used at analysis:

$$x'(n) = \alpha_{d_n} x(n) + \sum_j \beta_{d_n,j} y_j(n) , \qquad (4)$$

where $\beta_{d,j} = \alpha_d \lambda_{d,j}$.

In the next section, we shall be interested in finding sufficient conditions allowing to satisfy the *perfect reconstruction condition*, i.e., to recover $x(n)$ from $x'(n)$ and the original detail signal $y(n)$. Obviously, we can easily invert (4) through

$$x(n) = \frac{1}{\alpha_{d_n}} \left(x'(n) - \sum_j \beta_{d_n,j} y_j(n) \right) , \qquad (5)$$

presumed that the decision d_n is known at every location n. This shows that the inversion problem amounts to recovering (d_n) from x' and y. To simplify notations, we will henceforth omit n. In [8] it has been shown that a necessary condition for perfect reconstruction is that the value

$$\kappa_d = \alpha_d + \sum_j \beta_{d,j}$$

does not depend on d. Throughout the remainder of this paper we normalize the previous constants by setting $\kappa_0 = \kappa_1 = 1$.

3. QUADRATIC DECISION CRITERION

We define the gradient vector $\boldsymbol{v} = (v_{-L_1}, \ldots, v_{L_2})^T \in \mathbb{R}^N$, $N = L_2 + L_1 + 1$, by

$$v_k = x - y_k, \quad k = -L_1, \ldots, L_2 .$$

At synthesis, the gradient vector $\boldsymbol{v}' = (v'_{-L_1}, \ldots, v'_{L_2})^T$ will be computed in the same way, that is, $v'_k = x' - y_k$, $k = -L_1, \ldots, L_2$.

The decision map is assumed to depend exclusively on the gradient vector $\boldsymbol{v}$. Furthermore, we want to be able to recover the decision map at synthesis from $\boldsymbol{v}'$.

The decision rule is defined as

$$d = 1 \quad \text{if} \quad p(\boldsymbol{v}) > T \quad \text{and} \quad d = 0 \quad \text{otherwise.}$$

Here, p is a seminorm[1] and T denotes a given threshold. At synthesis, reconstruction of the decision map follows a similar rule, that is,

$$d = 1 \quad \text{if} \quad p(\boldsymbol{v}') > T' \quad \text{and} \quad d = 0 \quad \text{otherwise,}$$

where T' is a threshold related to T.

In our previous work [6, 8, 9], we have found perfect reconstruction conditions for various seminorms. In signal processing and control, it is however interesting to use criteria based on ellipsoidal confidence regions [10]. These confidence regions may for instance correspond to the fact that the likelihood of a Gaussian vector exceeds a given threshold. In this paper, we shall therefore consider a decision criterion based on a quadratic form of the components of the gradient vector:

$$p(\boldsymbol{v}) = \|\boldsymbol{v}\|_M = \left(\boldsymbol{v}^T M \boldsymbol{v}\right)^{1/2}, \qquad (6)$$

where M is a $N \times N$ non-zero symmetric positive semi-definite matrix.

The simplest example is the case where M reduces to the identity matrix, I. The decision criterion becomes $p(\boldsymbol{v}) = \|\boldsymbol{v}\|$ in this case. This is a very intuitive criterion, saying basically that the adaptation is based on the energy of the gradient of the input data. The matrix M introduces an additional degree of freedom, allowing to weight the different components of the gradient vector with parameters that can, for example, be tuned according to their relative distance to the sample to be updated.

Let r be the rank of M (we assume that $r > 1$), and denote by $\boldsymbol{u}$ the vector in $\mathbb{R}^N$ given by $\boldsymbol{u} = (1, 1, \ldots, 1)^T$. We obtain the following result [8]:

3.1 Proposition. *If p is given by (6), then perfect reconstruction is possible if one of the following two conditions are satisfied:*

1. $M\boldsymbol{u} = 0$;
2. $\boldsymbol{\beta}_d = \mu_d M \boldsymbol{u}$ *for* $d = 0, 1$, *where* μ_0, μ_1 *are such that*

$$|1 - \mu_0 S| \leq 1 \leq |1 - \mu_1 S| , \qquad (7)$$

where $S = \|u\|_M^2 = \sum_i \sum_j M_{ij}$.

Moreover we can choose $T' = T$ for the threshold at synthesis and this is the choice that we will use in our simulations.

We discuss some particular cases in more detail.

1. As seen before, if $M = I$, then p is the ℓ^2-norm. In this case (7) reduces to $|1 - \mu_0 N| \leq 1 \leq |1 - \mu_1 N|$, and $\beta_{d,j} = \mu_d$ for $d = 0, 1$ and all j.

[1] A seminorm is a function $p : \mathbb{R}^N \to \mathbb{R}_+$ with $p(\lambda \boldsymbol{v}) = |\lambda| p(\boldsymbol{v})$, and $p(\boldsymbol{v} + \boldsymbol{w}) \leq p(\boldsymbol{v}) + p(\boldsymbol{w})$ for $\boldsymbol{v}, \boldsymbol{w} \in \mathbb{R}^N$ and $\lambda \in \mathbb{R}$.

2. Assume that M is a diagonal matrix $M = \operatorname{diag}\big(m_{-L_1}, m_{-L_1+1}, \ldots, m_{L_2}\big)$ with r strictly positive diagonal terms m_j. By Prop. 3.1 we know that to guarantee perfect reconstruction, we must choose the filter coefficients in $\boldsymbol{\beta}_d$ collinear with vector $M\boldsymbol{u}$. This implies $\beta_{d,j} = \mu_d m_j$ and (7) reduces to $|1-\mu_0 \sum_j m_j| \leq 1 \leq |1-\mu_1 \sum_j m_j|$. Note that if $r < N$, this yields that $\beta_{d,j} = 0$ for all indices j with $m_j = 0$. In other words, the order of the update filter, initially assumed to be equal to N, is constrained to be at most r.

4. SIMULATION RESULTS

We first consider the case where the seminorm p is the weighted ℓ^2-norm, i.e, $p(\boldsymbol{v}) = (\sum_j m_j |v_j|^2)^{1/2}$. Let $L_1 = 2$, $L_2 = 1$ and $M = \operatorname{diag}\big(1/2, 1, 1, 1/2\big)$.

For low energy areas where $d = 0$, we choose μ_0 such that it minimizes the variance of the noise in the approximation signal, assuming an additive noise model for the original signal. If the noise is uncorrelated and Gaussian, it is easy to show that

$$\mu_0 = \frac{\sum_j m_j}{\sum_j m_j^2 + \big(\sum_j m_j\big)^2},$$

which in our case gives $\mu_0 = 6/23$. For $d = 1$, we choose $\mu_1 = 0$ (i.e., no modification of the approximation signal for high energy regions). Thus,

$$\boldsymbol{\beta}_0 = \frac{6}{23}(\frac{1}{2}, 1, 1, \frac{1}{2})^T,\ \alpha_0 = \frac{5}{23},\ \boldsymbol{\beta}_1 = \mathbf{0},\ \alpha_1 = 1\,.$$

The test signal (which is a fragment of the 'leleccum' data in Matlab wavelet toolbox) is shown in Fig. 2(a). After the polyphase decomposition, we apply the proposed adaptive update lifting, followed by a fixed prediction step of the form $y'(n) = y(n) - \frac{1}{2}(x'(n) + x'(n+1))$. The overall scheme is iterated over the approximation signal up to three levels. For each level, the approximation and the detail signals are depicted in Fig. 2(b) and Fig. 2(c) respectively. The decision map is also displayed in Fig. 2(b), where it has been represented as straight lines at those locations where $d = 1$. One can see that the adaptive scheme performs the smoothing determined by (4) except for those samples where the weighted energy of the gradient exceeds the threshold T. Such samples are considered as 'singularities' and the scheme 'decides' not to apply any smoothing. For comparison, we also show the decomposition signals obtained for the two corresponding non-adaptive cases using either U_0 (Fig. 2(d)-(e)) or U_1, (Fig. 2(f)-(g)), for the entire signal.

One can see that the adaptive scheme yields a smoothed approximation signal except near the discontinuities. The detail signal shows only a single peak near such discontinuities and avoids the oscillatory behaviour exhibited by the classical non-adaptive case.

To get an evaluation of the compression efficiency that can possibly be achieved by application of our adaptive scheme, we compute the entropies of the obtained decompositions in the adaptive and the two non-adaptive cases. We consider: (1) the entropy of the probability distribution of the decomposition; as well as the entropies based on (2) the normalized magnitude and (3) energy distribution [11]. Namely, given a sequence $\boldsymbol{x} = \{x_i\}_{i=1}^K$, we compute (1) as $h_0 = -\sum_{i=1}^K f(x_i) \log_2 f(x_i)$, where f is the histogram of $\boldsymbol{x}$; and (2), (3) (with $p = 1, 2$ respectively) as

$$h_p(\boldsymbol{x}) = -\sum_{i=1}^{K} \frac{|x_i|^p}{\|\boldsymbol{x}\|^p} \log_2 \frac{|x_i|^p}{\|\boldsymbol{x}\|_p^p},$$

where $\|\cdot\|_p$ refers to the ℓ^p-norm. In each case, the entropy is computed independently for each of the four signals (the approximation at the third level plus the three detail signals), scaled according to the number of samples of each signal, and finally added up. Table 1 shows that, for all these entropies, the adaptive scheme performs significantly better than the non-adaptive schemes.

	adaptive	$d=0$	$d=1$
h_0	9.993	11.189	10.588
h_1	12.473	13.137	12.832
h_2	7.457	9.671	8.489

Table 1. Entropy values for the adaptive (left), non-adaptive using U_0 (center) and non-adaptive using U_1 (right) decomposition schemes. Each row corresponds to a different entropy method computation.

5. CONCLUSION

In this paper, we have studied a nonlinear update lifting scheme driven by an automatic adaptation rule. Simulation tests show the capacity of the corresponding multiresolution decomposition in preserving the sharp transitions in the analysed signal, even at coarse resolution. The entropy reduction achieved by this new scheme is also a strong indication of its potential in data compression. Applications of this technique to image analysis are currently under investigation. In our future work we will also make a comparison between the various seminorms, including the quadratic seminorm used in this paper, that can be used in the decision rule triggering the update filter.

6. REFERENCES

[1] E. Le Pennec and S. Mallat, "Image compression with geometrical wavelets," in *Proceedings of the IEEE International Conference on Image Processing*, Vancouver, September 2000.

[2] D. L. Donoho, “Orthonormal ridgelets and linear singularities,” *SIAM Journal of Mathematical Analysis*, vol. 31, no. 5, pp. 1062–1099, 2000.

[3] E. Candès, “The curvelet transform for image denoising,” in *Proceedings of the IEEE International Conference on Image Processing*, Thessaloniki, Greece, October 2001.

[4] F. J. Hampson and J.-C. Pesquet, “M-band nonlinear subband decompositions with perfect reconstruction,” *IEEE Transactions on Image Processing*, vol. 7, pp. 1547–1560, 1998.

[5] H. J. A. M. Heijmans and J. Goutsias, “Nonlinear multiresolution signal decomposition schemes: Part II: morphological wavelets,” *IEEE Transactions on Image Processing*, vol. 9, no. 11, pp. 1897–1913, 2000.

[6] G. Piella and H. J. A. M. Heijmans, “Adaptive lifting schemes with perfect reconstruction,” Research Report PNA-R0104, CWI, 2001, to appear in IEEE Transactions on Signal Processing.

[7] W. Sweldens, “The lifting scheme: A new philosophy in biorthogonal wavelet constructions,” in *Wavelet Applications in Signal and Image Processing III*, A. F. Lain and M. Unser, Eds. Proceedings of SPIE, vol. 2569, 1995, pp. 68–79.

[8] H. J. A. M. Heijmans, B. Pesquet-Popescu, and G. Piella, “Nonredundant adaptive update lifting schemes,” Research Report, CWI, in preparation.

[9] B. Pesquet-Popescu, G. Piella, and H. J. A. M. Heijmans, “Adaptive update lifting with gradient criteria modeling high-order differences,” submitted to ICASSP 2002.

[10] A. Kurzhanski and I. Valyi, *Ellipsoidal calculus for Estimation and Control, Systems and Control: Fundations and Applications*, Birkhauser, Boston, 1997.

[11] V. M. Wickerhauser and R. R. Coifman, “Entropy-based algorithms for best basis selection,” *IEEE Transactions on Information Theory*, vol. 38, pp. 713–718, 1992.

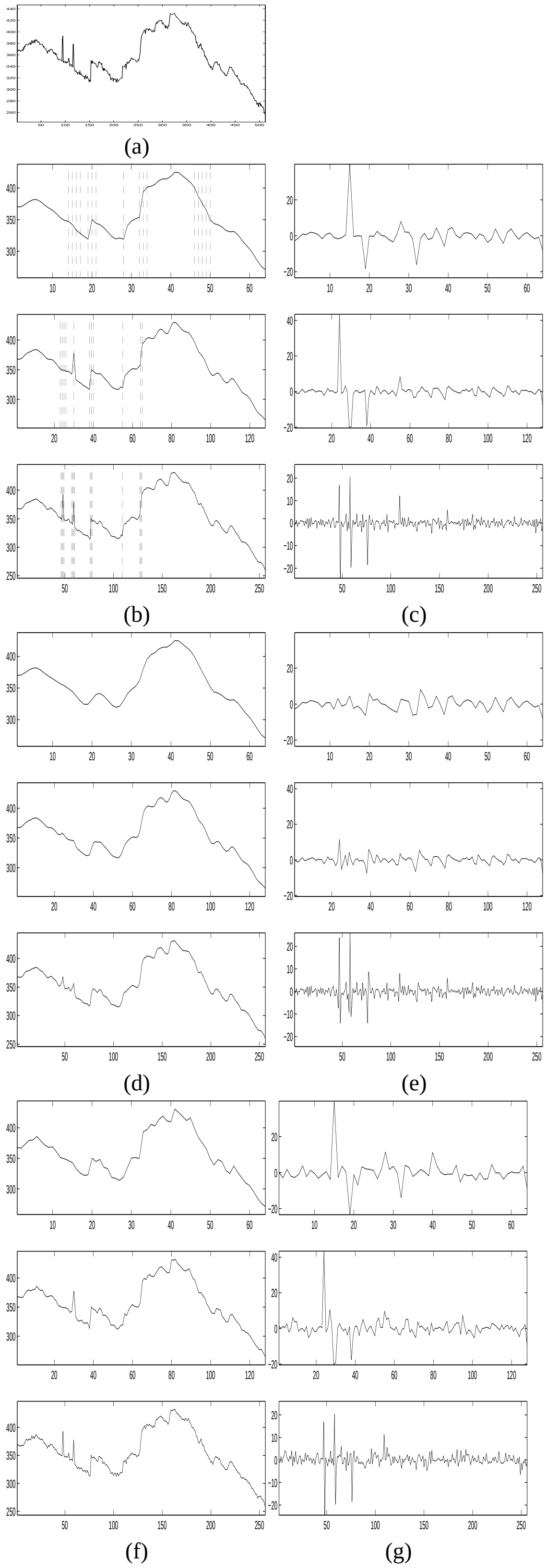

Fig. 2 (a) original signal; (b) adaptive,(d) non-adaptive $d = 0$ and (f) non-adaptive $d = 1$ approximation signals; (c) adaptive, (e) non-adaptive $d = 0$ and (g) non-adaptive $d = 1$ detail signals. In each case, the coarsest signal (3rd level) is displayed at the top, followed by the signals at levels 2 and 1. In (b), the straight lines indicate the locations where $d = 1$.